

# Temperature-Dependent Crystal Field and Charge Density: Mössbauer Studies of $\text{FeF}_2$ , $\text{KFeF}_3$ , $\text{FeCl}_2$ , and $\text{FeF}_3$ <sup>†</sup>

H. K. Perkins\* and Y. Hazony‡

*Department of Chemical Engineering, Princeton University, Princeton, New Jersey 08540*

(Received 24 May 1971)

A temperature-dependent crystal field at the  $\text{Fe}^{2+}$  site in  $\text{FeF}_2$  is inferred from anisotropic thermal-expansion coefficients and Mössbauer quadrupole-splitting data; the latter indicate that the splitting of the ferrous  $T_{2g}$  state, due to the axial component of the crystal field, decreases from  $E_{\text{axial}} = 1300$  °K at 300 °K to  $E_{\text{axial}} = 1000$  °K at 965 °K. Thermal-shift and thermodynamic data for  $\text{FeF}_2$ ,  $\text{KFeF}_3$ , and  $\text{FeCl}_2$  show that the electronic charge density at the nucleus is essentially independent of temperature; thus, the expected decrease in this density due to isothermal expansion must be approximately canceled by an increase due to thermal effects at constant volume. In contrast,  $\text{FeF}_3$  displays a significant decrease of electronic charge density at the nucleus with increasing temperature. The above conclusions result from Mössbauer studies of  $\text{Fe}^{57}$  in  $\text{FeF}_2$  (300–965 °K),  $\text{KFeF}_3$  (300–945 °K),  $\text{FeCl}_2$  (300–644 °K), and  $\text{FeF}_3$  (370–810 °K), reported in this paper. Also presented is a model which quantitatively fits the high-pressure  $\text{FeF}_2$  Mössbauer quadrupole-splitting data of Champion *et al.* below 60 kbar. The new feature of this model is a method for estimating the effect of pressure on the  $3d$  radial wave function. A phase transition is proposed around 65 kbar.

## I. INTRODUCTION

This paper consists of (i) a study of the temperature dependence of noncubic crystal fields as represented by  $\text{FeF}_2$ , (ii) a model for explaining the high-pressure quadrupole-splitting data on  $\text{FeF}_2$ , and (iii) an examination of the assumption that the electron density at the  $\text{Fe}^{57}$  nucleus has only an implicit temperature dependence due to thermal expansion. The iron  $3d$  electrons prove to be a sensitive probe of the environment, both via the splitting of the  $\text{Fe}^{2+}$   $T_{2g}$  state due to distortions from cubic symmetry and via the radial component of the  $3d$  wave function, which varies with covalency. The Mössbauer quadrupole splitting depends on the splitting of the  $T_{2g}$  state through a Boltzmann function, and on the  $3d$  radial distribution through the multiplicative  $\langle r^{-3} \rangle$  factor.<sup>1</sup> The measured shift of the Mössbauer resonance energy (or thermal shift) is the sum of the second-order Doppler shift, which depends on the mean square velocity of the  $\text{Fe}^{57}$  nucleus, and the isomer shift, which is proportional to the electron density at the  $\text{Fe}^{57}$  nucleus. (Only  $s$  electrons contribute to this density.)

Changes in the electron density at the nucleus result from the  $3s$ -electron radial function responding to changes in the shielding of the positive nucleus by the  $3d$  electrons. The electron density at the  $\text{Fe}^{57}$  nucleus has been found to increase both at higher pressures and in more covalent compounds, hence indicating an expansion of the  $3d$  orbitals.

Recent Mössbauer studies on  $\text{FeF}_2$  include (a) Ganiel and Shtrikman's analysis of their  $\text{FeF}_2$  quadrupole-splitting data (97–692 °K),<sup>2</sup> (b) Johnson and Ingalls's analysis of both  $\text{FeF}_2$  quadrupole-splitting and thermal-shift data (below 300 °K),<sup>3</sup>

and (c) Christoe and Drickamer's analysis of high-pressure quadrupole-splitting data.<sup>4</sup> The first two papers assumed that changes of quadrupole splitting with temperature resulted from the thermal population of fixed energy levels, while the last paper assumed that changes in the quadrupole splitting with pressure (at 300 °K) result from the thermal population of pressure-dependent energy levels: a dependence that arises because of the anisotropic compressibility of  $\text{FeF}_2$ .

This paper reports  $\text{FeF}_2$  quadrupole-splitting data (300–965 °K) which are not consistent with fixed energy levels or constant noncubic crystal fields. Our results indicate that two processes occur simultaneously: First, increases in temperature thermally populate the low-lying electron levels (in  $\text{FeF}_2$ ). This, in turn, changes the anisotropy of the  $3d$  electron charge density, thus affecting the crystal structure and energy separations between these low-lying levels. The evidence that these two processes occur together consists of Mössbauer quadrupole-splitting data and thermal-expansion data which we have previously discussed.<sup>5</sup>

Our model for explaining the high-pressure quadrupole-splitting data for  $\text{FeF}_2$  of Champion *et al.*<sup>6</sup> introduces a method for estimating changes in the expectation value  $\langle r^{-3} \rangle$  due to the radial expansion of the  $3d$  electrons at increased pressures. We propose a similarity between the decrease in  $\langle r^{-3} \rangle$  due to increased pressure and the decrease in  $\langle r^{-3} \rangle$  due to increased covalency in the anhydrous ferrous-halide compounds. This enables us to estimate the variation of  $\langle r^{-3} \rangle$  with pressure from the corresponding variation of the isomer shift using the proportionality constant observed for the ferrous halides.<sup>7</sup>

The thermal shift of the Mössbauer resonance energy ( $\delta E$ ) is analyzed as the sum of the second-order Doppler shift ( $\delta E_{\text{SOD}}$ ) described by an Einstein model and the isomer shift ( $\delta E_I$ ) assumed to vary linearly with temperature. The temperature dependence of the isomer shift will be discussed in terms of an implicit effect  $(\partial\delta E_I/\partial V)_T$  associated with volume expansion and an explicit effect  $(\partial\delta E_I/\partial T)_V$  due to possible constant-volume contributions from lattice vibrations, thermal population of low-lying states, etc.

Drickamer and co-workers<sup>4,6</sup> have demonstrated for numerous iron compounds that the Mössbauer resonance energy decreases when the lattice is compressed by an increase in pressure. This decrease is attributed to changes in the isomer shift and corresponds to an increase in *s*-electron density at the nucleus. This furnishes data for  $(\Delta\delta E_I/\Delta P)_T$  which allow the calculation of  $(\Delta\delta E_I/\Delta V)_T$  if the compressibility data are available. Several authors<sup>3,8</sup> have assumed that the temperature dependence of the isomer shift consists only of the implicit contribution given by  $(\partial\delta E_I/\partial V)_T \times (\partial V/\partial T)_P$  (due to volume expansion). Housely and Hess<sup>9</sup> have shown that this assumption is not true for metallic iron and its alloys; we present evidence that it is not true for certain iron compounds. Recently, Walsh *et al.*<sup>10</sup> and Shrivastava<sup>11</sup> have proposed an explicit thermal contribution to the changes of the *s*-electron density distribution produced by the increase of the vibrational amplitudes in the solid with increasing temperature. The evidence for an explicit temperature dependence presented in this paper consists of high-temperature thermal-shift data for three octahedral divalent iron compounds  $\text{FeF}_2$ ,  $\text{KFeF}_3$ , and  $\text{FeCl}_2$ , and the trivalent compound  $\text{FeF}_3$ , combined with the results of x-ray and high-pressure experiments, as well as thermodynamic data.

After describing the experimental details in Sec. II, we analyze the  $\text{FeF}_2$  nuclear quadrupole-splitting data in Sec. III. This includes (i) a review of the  $\text{FeF}_2$  crystal structure and the pertinent  $\text{Fe}^{2+}$  wave functions, (ii) a discussion of our high-temperature  $\text{FeF}_2$  quadrupole-splitting data, and (iii) a model for the high-pressure quadrupole-splitting data. Section IV includes the analysis of thermal-shift measurements on  $\text{FeF}_2$ ,  $\text{FeCl}_2$ ,  $\text{KFeF}_3$ , and  $\text{FeF}_3$  in order to obtain information on the temperature dependence of the isomer shift. For  $\text{FeF}_2$  it is possible to calculate the implicit (thermal-expansion) and explicit temperature dependences of the isomer shift using high-pressure Mössbauer data together with compressibility and thermal-expansion data. The slope of our thermal-shift data for  $\text{FeF}_3$  in the paramagnetic region, which are consistent with the data published by Wertheim *et al.*,<sup>8</sup> is significantly different from the

slope obtained for  $\text{FeF}_2$ . The assignment of this difference in slope to a difference in the isomer-shift contribution rather than a difference in the second-order Doppler shift<sup>8</sup> (as computed from lattice-specific-heat data) is also discussed. Section V contains a summary and discussion of our results.

## II. EXPERIMENTAL

Mössbauer transmission measurements were made on powdered absorbers contained in a Ricor Ltd. model MF-2 vacuum furnace where one could vary the temperature from 300 to 970 °K. A modified Elron constant-velocity spectrometer together with a temperature controller enabled both velocities and temperatures to be automatically changed. The Mössbauer data were simultaneously taken on IBM cards for computer analysis, and displayed on a two-channel chart recorder along with the voltage from a chromel-alumel thermocouple measuring the sample temperature. The compounds measured were  $\text{FeF}_2$  from two sources (Alfa Inorganics, Inc. and H. J. Guggenheim at Bell Telephone Laboratories),  $\text{KFeF}_3$  prepared by Vinor Laboratories,  $\text{FeF}_3$  from K & K Laboratories, and  $\text{FeCl}_2$  from Alfa Inorganics, Inc.

The Mössbauer source of  $\text{Co}^{57}$  diffused in Pd was held at room temperature. Initial experiments used a 1-mC source with later experiments using a 25-mC source, both obtained from New England Nuclear Corp. The velocity scale, which was calibrated with a natural iron foil several times during the experiments, has an estimated accuracy of 0.3%. All isomer shifts are referred to natural iron at room temperature.

The chromel-alumel thermocouple was calibrated at room temperature and at the antiferromagnetic-paramagnetic transition temperature of  $\text{Fe}_2\text{O}_3$  (948 °K)<sup>12</sup> by observing the Mössbauer resonance. With the velocity set on one of the paramagnetic peaks, the  $\gamma$ -ray transmission was recorded as the temperature passed through the transition. A sudden change in the  $\gamma$ -ray transmission was taken to indicate the transition temperature. Five measurements of the transition temperature gave values within  $\pm 2$  °K of the average value. The estimated error in temperature readings is less than  $\pm 4$  °K.

## III. ANALYSIS OF $\text{FeF}_2$ QUADRUPOLE-SPLITTING DATA

### A. $\text{FeF}_2$ Crystal Structure and $\text{Fe}^{2+}$ Wave Functions

In order to interpret our data certain known features of the  $\text{FeF}_2$  crystal structure and the associated  $\text{Fe}^{2+}$  wave functions are reviewed.  $\text{FeF}_2$  has the rutile crystal structure<sup>13</sup> with a tetragonal unit cell containing two  $\text{FeF}_2$  formula units. The  $\text{Fe}^{2+}$  ions occupy crystallographically equivalent sites at (0, 0, 0) and  $(\frac{1}{2}, \frac{1}{2}, \frac{1}{2})$ , while the  $\text{F}^-$  ions occupy

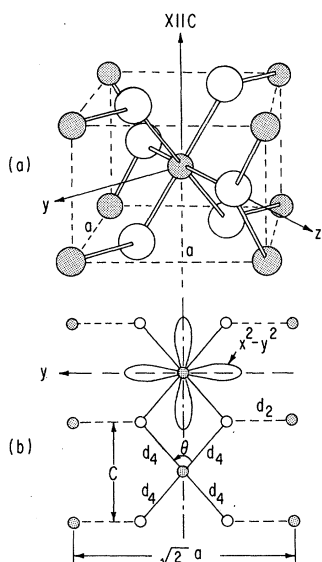


FIG. 1. (a) Orientation of the crystal field axes ( $x, y, z$ ) with respect to the tetragonal unit cell of the rutile structure. Filled circles correspond to cations and unfilled circles correspond to anions. (b) Atomic arrangement in the (110) plane ( $xy$  plane) with a sketch of the angular dependence of the  $d_{x^2-y^2}$  orbital for a body-centered cation. The distances between the four anions and body-centered cation ( $d_4$ ) are shown. The crystal field experienced by the corner cation differs from the body centered by a  $90^\circ$  rotation around the  $c$  axis. Consequently the  $d_2$  distance shown is identical with the distances to the two anions along the  $z$  axis (not shown).

sites at  $\pm(u, u, 0)$  and  $\pm(\frac{1}{2} + u, \frac{1}{2} - u, \frac{1}{2})$ . The  $\text{Fe}^{2+}$  ion is surrounded by a distorted octahedron of  $6\text{F}^-$  ions (Fig. 1) having the Fe-F bond distances ( $d_2, d_4$ ) and the rhombic angle  $\theta$  shown in Table I. Variations in  $d_2, d_4$  and  $\theta$  with either temperature or pressure affect the quadrupole splitting of the  $\text{Fe}^{57}$  nucleus by two mechanisms: (a) changing the orthorhombic splitting of the  $T_{2g}$   $\text{Fe}^{2+}$  electronic ground state and (b) changing the value of  $\langle r^{-3} \rangle_{3d}$  due to covalency effects. Changes in  $\langle r^{-3} \rangle_{3d}$  affect the shielding of the  $3s$  electrons from the  $\text{Fe}^{57}$  nucleus and thereby affect the isomer shift. X-ray measurements of the lattice parameters as a function of pressure by Christoe *et al.*<sup>4</sup> indicate anisotropic compressibility as demonstrated by the varying  $a/c$  ratio in Fig. 2. High-temperature x-ray

TABLE I.  $\text{FeF}_2$  crystal parameters.

$T$ ( $^\circ\text{K}$ )	$a$ ( $\text{\AA}$ )	$c$ ( $\text{\AA}$ )	$u$	$d_2$ ( $\text{\AA}$ )	$d_4$ ( $\text{\AA}$ )	$\theta$ (deg)
300	4.697	3.309	0.300	1.993	2.122	78
722	4.740	3.300	0.300 <sup>a</sup>	2.011 <sup>a</sup>	2.126 <sup>a</sup>	83 <sup>a</sup>

<sup>a</sup>The fluoride parameter  $u$  is assumed to be equal to the  $300^\circ\text{K}$  value.

measurements by Krishna Rao *et al.*<sup>14</sup> show that  $\text{FeF}_2$  not only exhibits anisotropic thermal expansion as indicated by a varying  $a/c$  ratio (Fig. 2), but actually has a negative thermal-expansion coefficient along the  $c$  axis (Fig. 3). Elsewhere<sup>5</sup> we have proposed a model to explain the negative thermal expansion and in this paper shall only consider its effect on the surroundings of the  $\text{Fe}^{2+}$  ion. In order to calculate  $d_2, d_4$  and  $\theta$  from the available high-temperature x-ray data ( $a$  and  $c$ ) we assumed that the fluoride parameter  $u$  does not change with temperature<sup>15</sup> and obtained the values shown in Table I. The difference in Fe-F distances ( $d_4 - d_2$ ) has decreased by 11% at  $722^\circ\text{K}$  relative to its  $300^\circ\text{K}$  value and the rhombic angle  $\theta$  differs from the octahedral value of  $90^\circ$  by  $7^\circ$  at  $722^\circ\text{K}$  compared with  $12^\circ$  at  $300^\circ\text{K}$ . Hence, one expects a decrease in the orthorhombic component of the crystal field at high temperatures. An examination of Christoe's calculation<sup>4</sup> of  $d_2, d_4$  and  $\theta$  from his measured  $a$  and  $c$  parameters at high pressures shows that he made the tacit assumption of constant  $u$ —an assumption that we question at higher pressures where the unit-cell distortion  $a/c$  would produce a 50% de-

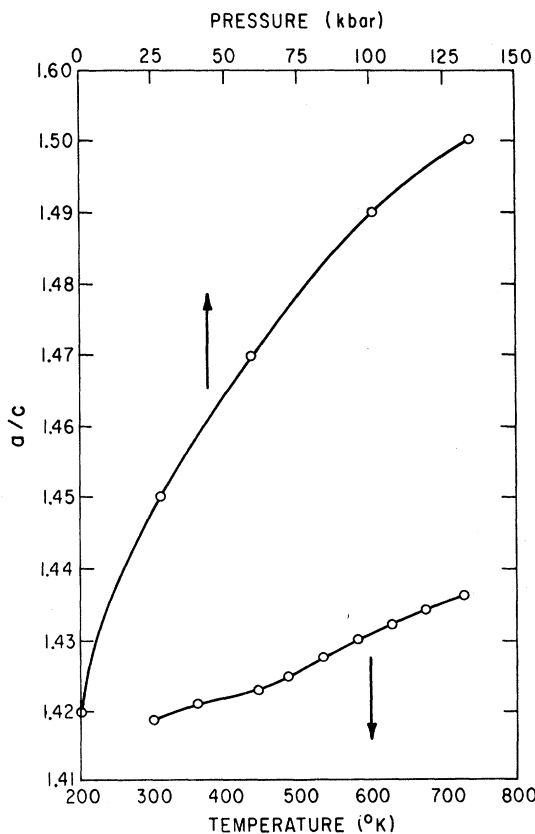


FIG. 2. Ratio of the  $\text{FeF}_2$  tetragonal unit-cell parameters as a function of temperature and pressure. The ratios are calculated using data reported by Christoe and Drickamer (Ref. 4) and Krishna Rao *et al.* (Ref. 14).

crease in the difference  $d_4 - d_2$ . Intuitively one does not expect  $u$  to remain unchanged over such a wide range.<sup>15</sup> In fact, the experimental quadrupole-splitting suggests that  $u$  may change around 60 kbar where  $d_4 - d_2$  has decreased by 25%.

The octahedral crystal field splits the free-ion  $\text{Fe}^{2+}$  ground term  ${}^5D$  into a low-lying triplet  $T_{2g}$  and a higher doublet  $E_g$  separated by 8800  $\text{cm}^{-1}$ .<sup>16</sup> The five  $d$ -orbital wave functions for  $\text{Fe}^{2+}$  appropriate to its rhombic symmetry ( $mmm$ ) using the axes in Fig. 1 are

$$\begin{aligned}\psi_1 &= \alpha |x^2 - y^2\rangle + \beta |3z^2 - r^2\rangle, \\ \psi_2 &= |yz\rangle, \\ \psi_3 &= |xz\rangle, \\ \psi_4 &= |xy\rangle, \\ \psi_5 &= -\beta |x^2 - y^2\rangle + \alpha |3z^2 - r^2\rangle.\end{aligned}\quad (1)$$

With this nonstandard choice of axes (due to the rhombic-site symmetry) the  $T_{2g}$  wave functions are  $|x^2 - y^2\rangle$ ,  $|yz\rangle$ , and  $|xz\rangle$ , and the  $E_g$  wave functions

$$f(E_2, E_3, T) = \frac{[1 + e^{-2E_2/T} + e^{-2E_3/T} - e^{-(E_2+E_3)/T} - (\alpha^2 - 2\sqrt{3}\alpha\beta - \beta^2)e^{-E_2/T} - (\alpha^2 + 2\sqrt{3}\alpha\beta - \beta^2)e^{-E_3/T}]^{1/2}}{1 + e^{-E_2/T} + e^{-E_3/T}}. \quad (3)$$

Here we have included only the predominant valence contribution to the quadrupole splitting. The scaling parameter  $Q \langle r^{-3} \rangle (1 - R)$ , which is the product of the nuclear quadrupole moment  $Q$ ,  $\langle r^{-3} \rangle$  of the  $3d$  electron and the Sternheimer antishielding factor  $(1 - R)$ , is determined indirectly by calibrating our calculations to the measured results of Wertheim and Buchanan<sup>17</sup> at 78.2 °K ( $\Delta E_Q = 2.92$  mm/sec), where only  $\psi_1$  is significantly occupied. (The negligible temperature dependence of  $\langle r^{-3} \rangle$  is estimated later.) The value of 0.11 is chosen for  $|\beta/\alpha|$  consistent with the low-temperature measurements of the asymmetry parameter  $\eta$ .<sup>2,17</sup> A least-squares search with  $|\beta/\alpha| = 0.11$  and  $\lambda = 0$  for the best fit of our data to Eq. (2) gives  $E_{\text{axial}} = \frac{1}{2}(E_2 + E_3) = (1180 \pm 250)$  °K and  $E_{\text{rhombic}} = E_3 - E_2 = (140 \pm 1000)$  °K.

The error limits given by our least-squares fit show that (i) our experimental data are not consistent with a constant  $E_{\text{axial}}$  and (ii) the large error limits on  $E_{\text{rhombic}}$  represent the insensitivity of  $\Delta E_Q$  to this parameter [e.g., changing  $E_{\text{rhombic}} = 150$  °K by  $\pm 150$  °K produces changes in the  $\Delta E_Q(T)$  curves in Fig. 4 at  $T > 300$  °K equivalent to changing  $E_{\text{axial}}$  by  $\mp 25$  °K]. A comparison of the experimental data and calculated  $\Delta E_Q(T)$  curves suggests that  $E_{\text{axial}}$  changes from 1300 to 1175 °K (a decrease of 9%) as the temperature increased from 300 to 722 °K. This should be compared with the decrease in the difference between the two Fe-F distances

are  $|xy\rangle$  and  $|3z^2 - r^2\rangle$ .  $\psi_1$  and  $\psi_5$  result from the mixing of the  $T_{2g} |x^2 - y^2\rangle$  state and the  $E_g |3z^2 - r^2\rangle$  state by the rhombic perturbation with  $\beta/\alpha$  expected to be small since the cubic splitting is large. The states  $\psi_i$  (which are exact eigenstates only for a zero spin-orbit coupling constant  $\lambda$ ) are used because the spin-orbit coupling produces a small effect on the quadrupole splitting ( $\lambda \sim 85$   $\text{cm}^{-1}$ ).<sup>2,3</sup>  $\psi_1$  is chosen as the ground state, in agreement with recent papers,<sup>2,3</sup> even though a simple point-charge calculation<sup>4</sup> using the six nearest  $\text{F}^-$  ions predicts  $\psi_2$  to be the ground state.

#### B. Temperature Variation of Quadrupole Splitting

The experimental quadrupole splitting is shown in Fig. 4 together with a family of calculated curves  $\Delta E_Q(T)$  which thermally average the contribution from the  $T_{2g}$  states ( $\psi_1, \psi_2, \psi_3$ ) according to the formula

$$\Delta E_Q(T) = \frac{2}{7} e^2 Q (1 - R) \langle r^{-3} \rangle f(E_2, E_3, T), \quad (2)$$

where

of 11% over the same temperature range (Table I). Several attempts to fit the data with a constant  $E_{\text{axial}}$  were unsuccessful; in particular we tried (a) considering a temperature dependence in  $\langle r^{-3} \rangle$  based on the isomer-shift data as discussed in Sec. III C; (b) examining the effect of changing  $E_{\text{rhombic}}$  (including  $E_{\text{rhombic}} = 1000$  °K); and (c) including the lattice electric field gradient calculated by Johnson and Ingalls.<sup>3</sup> The weak dependence of  $\Delta E_Q(T)$  on  $E_{\text{rhombic}}$  prevents any conclusion being drawn about its temperature dependence although the x-ray data (assuming constant  $u$ ) indicate that it should also decrease.

#### C. Pressure Variation of Quadrupole Splitting

Using Eq. (2) one can write the differential of  $\Delta E_Q$  in terms of differentials of  $\langle r^{-3} \rangle$  and  $f(E_2, E_3, T)$ :

$$d\Delta E_Q = \frac{2}{7} e^2 Q (1 - R) [f(E_2, E_3, T) d\langle r^{-3} \rangle + \langle r^{-3} \rangle df(E_2, E_3, T)], \quad (4)$$

with the nuclear quadrupole moment  $Q$  and the Sternheimer factor  $(1 - R)$  assumed to be constant.<sup>18</sup> The magnitude of the first term in Eq. (4) may be estimated from the pressure dependence of the isomer shift using the phenomenological relationship of Axtmann *et al.*<sup>7</sup> appropriate to the anhydrous ferrous halides. They observe that the linear re-

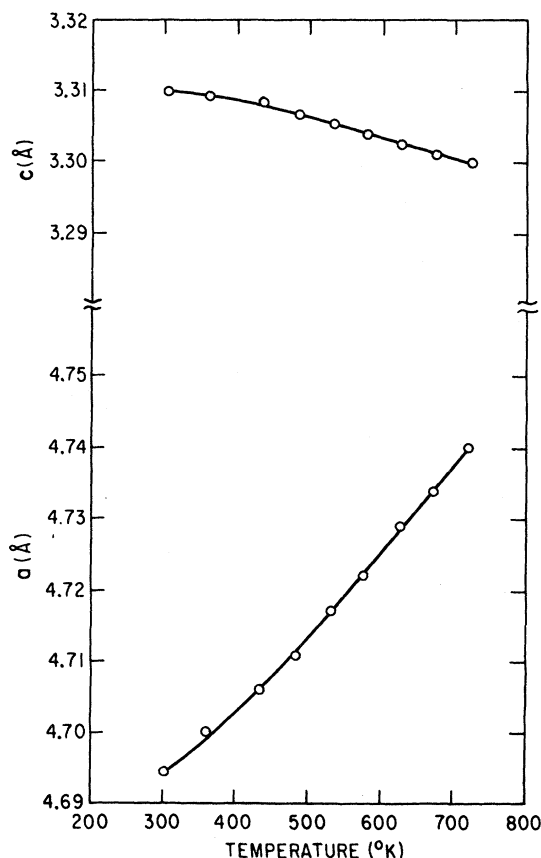


FIG. 3.  $\text{FeF}_2$  tetragonal unit-cell parameters ( $a, c$ ) as a function of temperature. Note that  $c$  decreases with increasing temperature. The data were reported by Krishna Rao *et al.* (Ref. 14).

lation between the experimental isomer shift and quadrupole splitting (corrected for degeneracy) at low temperatures gives a phenomenological relation

$$\frac{2}{7} e^2 Q(1-R)f(E_2, E_3, T) d \langle r^{-3} \rangle = 3.2 \delta \delta E_I. \quad (5)$$

We propose that Eq. (5) holds at higher temperatures where  $f(E_2, E_3, T)$  changes also contribute to  $\Delta E_Q$  variation, and that such a relationship describes the effects of compression or expansion on covalency.

The pressure dependence of the quadrupole splitting of  $\text{Fe}^{57}$  in  $\text{FeF}_2$  measured by Champion *et al.*<sup>6</sup> is shown in Fig. 5 together with several sets of calculated points based on experimental data. We used the isomer-shift data<sup>6</sup> and Eq. (5) to estimate the effect of pressure on  $\langle r^{-3} \rangle$  and on the quadrupole splitting, assuming that  $f(E_2, E_3, T)$  remains constant. On the other hand, Christoe and Drickamer<sup>4</sup> used their x-ray data to estimate the changes in  $E_2$  and  $E_3$  via  $f(E_2, E_3, T)$ , assuming that  $\langle r^{-3} \rangle$  remains constant. They made a point-charge calculation of the crystal field at the  $\text{Fe}^{2+}$  ion based on

the positions of six nearest fluoride ions. The arrangement of the  $\text{F}^-$  ions as described by  $d_2, d_3$ , and  $\theta$  (Fig. 1) is based on x-ray measurements of the lattice parameters ( $a, c$ ) and the tacit assumption that  $u(0.300)$  remains unchanged with pressure.<sup>15</sup> The failure of either of Christoe and Drickamer's models to fit the experimental data is due to (i) ignoring the significant effect of  $\langle r^{-3} \rangle$  change and (ii) a possible phase transition around 65 kbar inferred from the factor-of-20 change in the slope of the experimental quadrupole splitting. Since the lattice parameters ( $a, c$ ) show no anomaly near 65 kbar, we suggest that changes in the unmeasured parameter  $u$  occur and that above 65 kbar Christoe and Drickamer's models based on constant  $u$  cease to be valid. A decrease in  $u$  of 0.005 would account for this. The daggers in Fig. 5 show our calculated values of  $\Delta E_Q$  for  $P < 65$  kbar obtained by summing the effects of  $\langle r^{-3} \rangle$  and energy-level changes as calculated by Christoe and Drickamer with  $\psi_1$  as the ground state. No  $\Delta E_Q$  values are calculated above 65 kbar since we do not have enough information to calculate a  $f(E_2, E_3, T)$  contribution consistent with the factor-of-20 change in the experimental slope.

Now let us examine the validity of assuming in

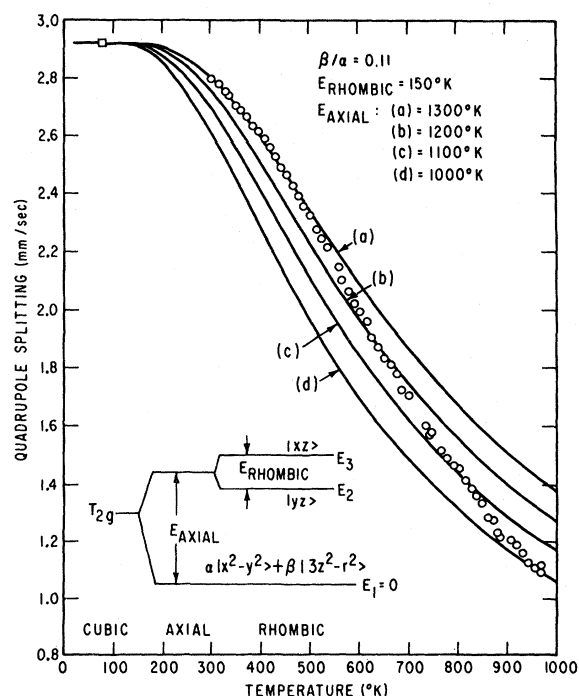


FIG. 4. Quadrupole splitting of  $\text{FeF}_2$  as a function of temperature. The curves are calculated using Eq. (2); the open circles are our data, the closed square is the data of Wertheim *et al.* (Ref. 17), and the insert shows the crystal field splitting of the  $\text{Fe}^{2+}$  cubic-field ground state. Our experimental error increases from  $\pm 0.005$  mm/sec at 300 °K to  $\pm 0.008$  mm/sec at 900 °K.

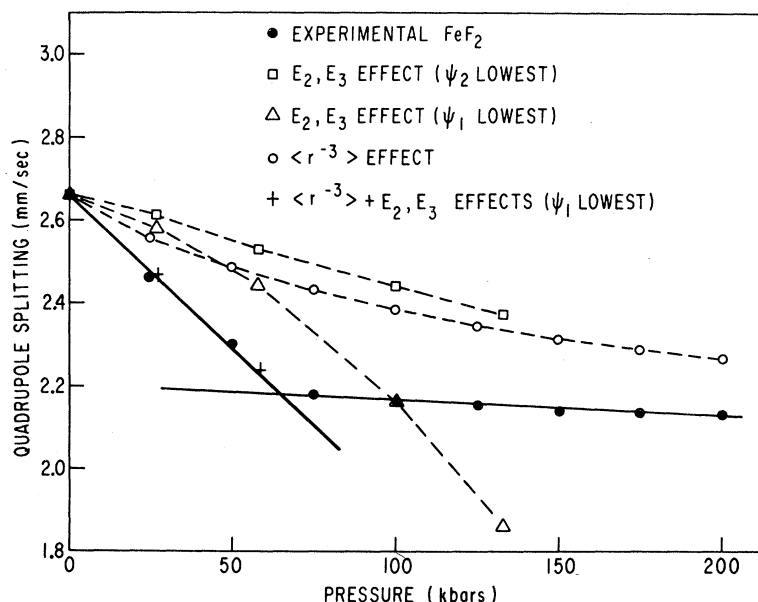


FIG. 5. Quadrupole splitting of  $\text{FeF}_2$  as a function of pressure. We have chosen to fit the experimental data of Champion *et al.* (Ref. 6) with two straight lines; the point size corresponds to a variation of  $\pm 1$  in their last reported digit. The squares and triangles correspond to calculations by Christoe and Drickamer (Ref. 4). The open circles and crosses are calculated using Eqs. (4) and (5).

Sec. III B that the experimental high-temperature quadrupole splitting only depends on  $df$  changes. As we will see in Sec. IV,  $\delta E_I$  decreases by 0.008 mm/sec as the temperature increases from 300 to 965 °K. The expected decrease in  $\Delta E_Q$  from  $d\langle r^{-3} \rangle$  is 0.026 mm/sec compared with an experimental decrease in the quadrupole splitting of 1.8 mm/sec. This value of 0.026 mm/sec is also small compared with the 0.3 mm/sec contribution to  $\Delta E_Q$  at 965 °K, previously attributed to a decrease in  $E_2$  and  $E_3$ . Hence, we conclude that the effect on  $\Delta E_Q$  from changes in  $\langle r^{-3} \rangle$  with temperature is negligible, even though changes in  $\langle r^{-3} \rangle$  account for 50% of the decrease in the quadrupole splitting of  $\text{FeF}_2$  at

high pressures.

#### IV. ANALYSIS OF THERMAL-SHIFT DATA

##### A. Thermal Shift of $\text{FeF}_2$

The thermal shift  $\delta E$  of the Mössbauer spectrum is the sum of the second-order Doppler shift  $\delta E_{\text{SOD}}$  and isomer shift  $\delta E_I$ ,

$$\delta E = \delta E_{\text{SOD}} + \delta E_I. \quad (6)$$

The isomer shift is a measure of the electron density at the  $\text{Fe}^{57}$  nucleus while the second-order Doppler shift varies linearly with the mean square velocity of the  $\text{Fe}^{57}$  nucleus. Our experimental thermal-shift values on  $\text{FeF}_2$  are shown in Fig. 6

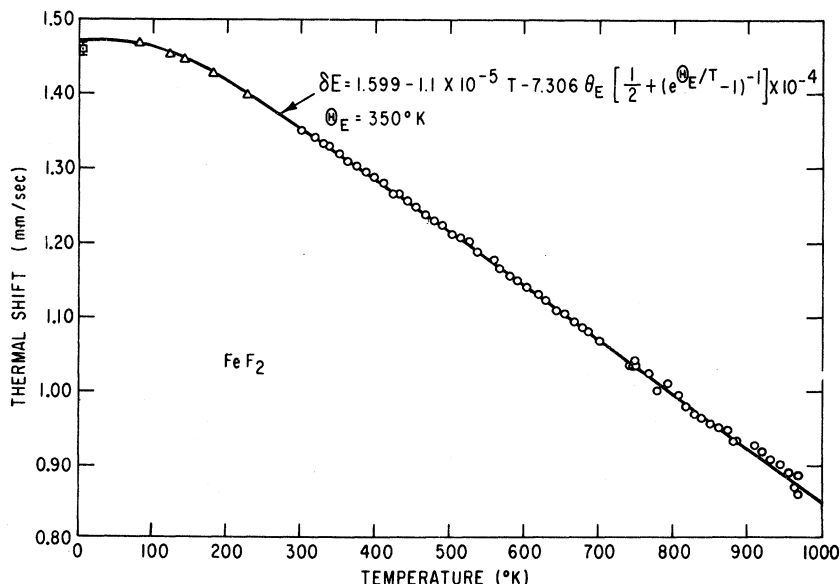


FIG. 6. Mössbauer resonance energy of  $\text{FeF}_2$  as a function of temperature. The square represents the data of Wertheim *et al.* (Ref. 17), the triangles represent the data of Johnson and Ingalls (Ref. 3), and the circles represent our data. Our experimental error increases from  $\pm 0.005$  mm/sec at 300 °K to  $\pm 0.010$  mm/sec at 965 °K.

together with the best least-squares fit by a computer to the formula

$$F(T) = \delta E_I^0 + \epsilon \times 10^{-5} T - 7.306 \Theta_E \times \left[ \frac{1}{2} + (e^{\Theta_E/T} - 1)^{-1} \right] \times 10^{-4} \text{ mm/sec } ^\circ\text{K}. \quad (7)$$

Here  $\delta E_I^0$  is the isomer shift at  $0^\circ\text{K}$ ,  $\epsilon$  is a linear approximation for the isomer-shift change due to both increased volume (thermal expansion) and any explicit temperature dependence  $(\partial \delta E_I / \partial T)_V$ , and  $\Theta_E$  is the Einstein temperature appropriate to using the Einstein model to calculate the temperature dependence of the mean square velocity of  $\text{Fe}^{57}$ . The calculated parameters

$$\begin{aligned} \delta E_I^0 &= 1.599 \pm 0.012 \text{ mm/sec}, \\ \epsilon &= -1.1 \pm 1.0 \text{ mm/sec } ^\circ\text{K}, \\ \Theta_E &= (350 \mp 78) ^\circ\text{K}, \end{aligned}$$

have large error limits due to correlation between  $\Theta_E$  and  $\epsilon$  in determining the slope, and  $\delta E_I^0$  and  $\Theta_E$  in determining the intercept. A visual comparison of the experimental data and plots of Eq. (7) using the best  $\Theta_E$  and  $\delta E_I^0$  values for the assumed  $\epsilon$  gives similar results. The curves fit the experimental data with  $\epsilon = -0.5, -1.1, -1.5$ , and  $-2.0$  and show a systematic deviation from the experimental data for  $\epsilon \geq 0.0$  and  $\epsilon \leq -2.5$ , thus supporting the computer-estimated value of  $\epsilon = -1.1 \pm 1.0$ . Johnson and Ingalls<sup>3</sup> report their low-temperature data ( $T < 300^\circ\text{K}$ ) to fit Eq. (7) with  $\delta E_I^0 = 1.348$  (relative to their source),  $\epsilon = 2.5$ , and  $\Theta_E = 270^\circ\text{K}$ ; however, this does not fit our high-temperature data. Figure 6 shows that their data fit the curve calculated for our high-temperature data.

The negative value for  $\epsilon$  suggests an explicit temperature dependence  $(\partial \delta E_I / \partial T)_V$  in addition to the more commonly considered positive implicit temperature dependence arising from thermal expansion. For  $\text{FeF}_2$  we can calculate the explicit temperature dependence of the isomer shift if we assume isotropic thermal expansion and compression (which Fig. 2 shows to be untrue), and partial derivatives which do not change over the temperature and pressure range ( $300\text{--}722^\circ\text{K}$ ,  $0\text{--}25$  kbar). Then the appropriate formulas are

$$\left( \frac{\partial \delta E_I}{\partial T} \right)_P = \left( \frac{\partial \delta E_I}{\partial T} \right)_V + \left( \frac{\partial \delta E_I}{\partial \ln V} \right)_T \left( \frac{\partial \ln V}{\partial T} \right)_P \quad (8)$$

and

$$\left( \frac{\partial \delta E_I}{\partial \ln V} \right)_T = \left( \frac{\partial \delta E_I}{\partial P} \right)_T \left( \frac{\partial P}{\partial \ln V} \right)_T \quad (9)$$

Using the values

$$\left( \frac{\partial \delta E_I}{\partial T} \right)_P = -1.1 \times 10^{-5} \text{ mm/sec } ^\circ\text{K},$$

$$\left( \frac{\partial \ln V}{\partial T} \right)_P = 3.9 \times 10^{-5} / ^\circ\text{K},$$

$$\left( \frac{\partial \ln V}{\partial P} \right)_T = 1.0 \times 10^{-3} / \text{kbar},$$

$$\left( \frac{\partial \delta E_I}{\partial P} \right)_T = 1.3 \times 10^{-3} \text{ mm/sec kbar}$$

calculated from our experiments together with the x-ray measurements of Christoe<sup>4</sup> and Krishna Rao *et al.*<sup>14</sup> (Fig. 3) and the high-pressure Mössbauer measurements of Champion *et al.*,<sup>6</sup> we estimate the explicit temperature dependence

$$\left( \frac{\partial \delta E_I}{\partial T} \right)_V = -(6 \pm 1) \times 10^{-5} \text{ mm/sec } ^\circ\text{K}$$

based on a calculated implicit temperature dependence

$$\left( \frac{\partial \delta E_I}{\partial \ln V} \right)_T \left( \frac{\partial \ln V}{\partial T} \right)_P = +5 \times 10^{-5} \text{ mm/sec } ^\circ\text{K}.$$

The calculated implicit temperature dependence is twice as large as that estimated by Johnson and Ingalls.<sup>3</sup>

#### B. Thermal Shift of $\text{KFeF}_3$

The  $\text{Fe}^{2+}$  ion in  $\text{KFeF}_3$ , which has the cubic perovskite structure, is surrounded by an undistorted octahedron of  $6\text{F}^-$  ions at a distance of  $2.06 \text{ \AA}$ .<sup>19,20</sup> Figure 7 shows the measured thermal shift at  $\text{KFeF}_3$  which was analyzed by a least-squares fit to Eq. (7) to give

$$\begin{aligned} \delta E_I^0 &= 1.593 \pm 0.011 \text{ mm/sec}, \\ \epsilon &= -0.8 \pm 1.0 \text{ mm/sec } ^\circ\text{K}, \\ \Theta_E &= (413 \pm 60) ^\circ\text{K}. \end{aligned}$$

Thus  $\epsilon$  behaves alike for both  $\text{FeF}_2$  and  $\text{KFeF}_3$ , even though in  $\text{FeF}_2$  the  $T_{2g}$  state of  $\text{Fe}^{2+}$  is split due to the rhombic crystal field, while in  $\text{KFeF}_3$  the  $T_{2g}$  state of  $\text{Fe}^{2+}$  is unsplit in the cubic crystal field.

Next we would like to estimate the contribution to  $\epsilon$  from volume expansion. X-ray data of Okazaki and Suemune<sup>20</sup> for  $\text{KFeF}_3$  below  $300^\circ\text{K}$  were used to estimate a volume thermal-expansion coefficient of  $4.4 \times 10^{-5} / ^\circ\text{K}$  compared with  $3.4 \times 10^{-5} / ^\circ\text{K}$  for  $\text{FeF}_2$  at  $350^\circ\text{K}$ . The high-pressure isomer-shift data are similar to  $\text{FeF}_2$ <sup>6</sup>; however, compressibility data are not available. Nevertheless, it seems reasonable to assume a volume contribution to  $\epsilon$  that is within a factor of 2 of the value calculated for  $\text{FeF}_2$ . This would imply that  $\text{KFeF}_3$  also has a negative explicit temperature dependence of its isomer shift which approximately cancels the contribution from volume expansion.

#### C. Thermal Shift of $\text{FeCl}_2$

$\text{FeCl}_2$  has the  $\text{CdCl}_2$  structure with  $\text{Fe}^{2+}$  sur-

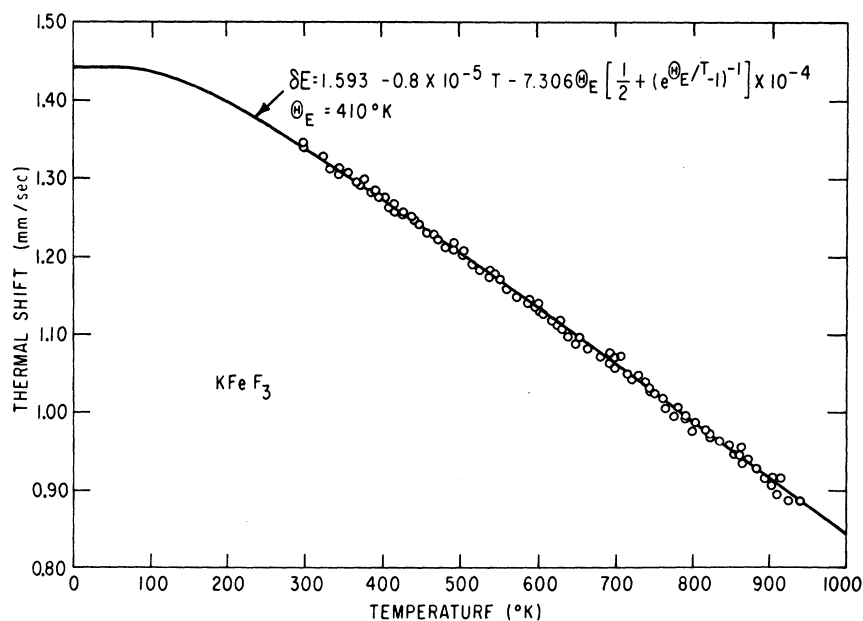


FIG. 7. Mössbauer resonance energy of  $\text{KFeF}_3$  as a function of temperature. The experimental error increases from  $\pm 0.005$  mm/sec at  $300^\circ\text{K}$  to  $\pm 0.008$  mm/sec at  $940^\circ\text{K}$ .

rounded by a trigonally distorted octahedron of  $\text{Cl}^-$  ions.<sup>19</sup> Our thermal-shift data for  $\text{FeCl}_2$ , shown in Fig. 8, were analyzed as before by a least-squares fit of Eq. (7), except that  $\Theta_E$  was held fixed at  $140^\circ\text{K}$ , as obtained by Hazony *et al.*<sup>21</sup> from their low-temperature isomer-shift data. The calculated parameters are

$$\delta E_I^0 = 1.314 \pm 0.001 \text{ mm/sec},$$

$$\epsilon = 0.11 \pm 0.24 \text{ mm/sec } ^\circ\text{K}.$$

(Using  $\Theta_E$  fixed at  $170^\circ\text{K}$  as reported by Johnson and Dash,<sup>22</sup> the  $\delta E_I^0$  and  $\epsilon$  values were  $1.316 \pm 0.001$  mm/sec and  $-0.2 \pm 0.3$  mm/sec  $^\circ\text{K}$ , respectively.) Our improved error limits arise because  $\Theta_E$  is held fixed instead of allowed to vary as before. Comparison of the small  $\epsilon$  value of  $0.1$  mm/sec  $^\circ\text{K}$  with typical predicted  $\epsilon \approx 3$  mm/sec  $^\circ\text{K}$  due to volume expansion suggests that  $\text{FeCl}_2$  also has a negative explicit temperature dependence of its isomer shift which cancels the effect of volume expansion. We certainly expect a contri-

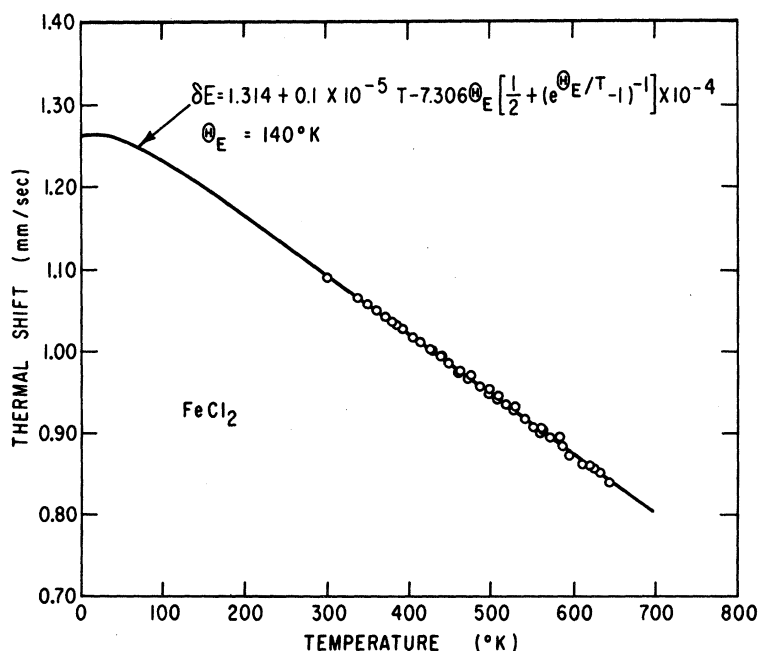


FIG. 8. Mössbauer resonance energy of  $\text{FeCl}_2$  as a function of temperature. The experimental error increases from  $\pm 0.005$  mm/sec at  $300^\circ\text{K}$  to  $\pm 0.008$  mm/sec at  $640^\circ\text{K}$ .



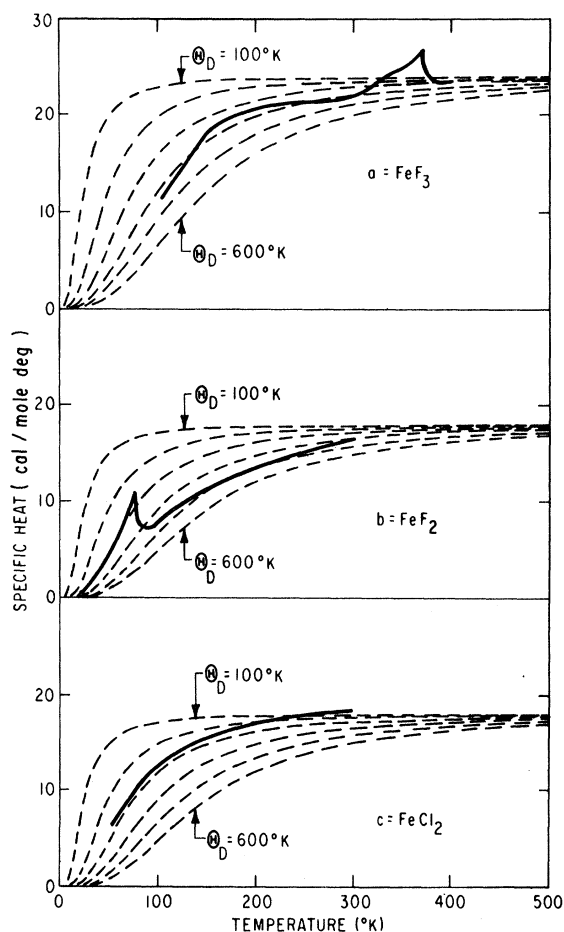


FIG. 9. Specific-heat curves as a function of temperature. The solid curves represent experimental data at constant pressure with the  $\text{FeF}_3$  data reported in Ref. 25, the  $\text{FeF}_2$  data reported in Ref. 26, and the  $\text{FeCl}_2$  data reported in Ref. 23. The dashed curves represent specific-heat curves at constant volume calculated using a Debye model for the Debye temperature  $\Theta_D$  equal to 100, 200, 300, 400, 500, and 600 °K.

tribution to the isomer shift from thermal expansion since a large degree of anharmonicity has been observed by analyzing the Mössbauer data.<sup>21,22</sup> Also, the fact that the specific-heat data for  $\text{FeCl}_2$ <sup>23</sup> in Fig. 9 are appreciably above the limiting value of Dulong and Petit indicates the effect of thermal expansion associated with the lattice anharmonicity.

In the Appendix is a tabulation of our experimental quadrupole data, which are consistent with the values reported by Ono *et al.*<sup>24</sup> at 430 and 530 °K, but are much more complete and have lower error limits.

#### D. Thermal Shift of $\text{FeF}_3$

Next let us compare the temperature shifts of the Mössbauer resonance energy of  $\text{FeF}_2$  and  $\text{FeF}_3$  above 363 °K, the Néel temperature for  $\text{FeF}_3$ . We

analyzed our data by a least-squares fit to a linear model since the temperature range proved to be insufficient to use Eq. (7). Reference to Fig. 10 shows that  $\text{FeF}_2$  has a more negative slope than  $\text{FeF}_3$ ; a fact which implies a larger Debye temperature  $\Theta_D$  for  $\text{FeF}_3$  or a different isomer-shift coefficient than found for  $\text{FeF}_2$ .

Wertheim *et al.*<sup>8</sup> have recently analyzed their  $\text{FeF}_3$  thermal-shift data from 4 to 700 °K in terms of two models: (a) a constant Debye temperature  $\Theta_D$  and a zero isomer-shift coefficient ( $\epsilon$ ), or (b) a magnetization-dependent  $\Theta_D$  and  $\epsilon = 1.5 \text{ mm/sec } ^\circ\text{K}$ . A good fit is obtained for model (a) with  $\Theta_D = 615$  °K or for model (b) with  $\Theta_D = (506 \pm 80)$  °K in the paramagnetic region. Our data are in good agreement with theirs; however, we wish to compare their Debye temperatures with the specific-heat Debye temperature.

Figure 9 shows the experimental specific-heat data ( $C_p$ ) for  $\text{FeF}_3$ ,<sup>25</sup>  $\text{FeF}_2$ ,<sup>26</sup> and  $\text{FeCl}_2$ <sup>23</sup> superimposed on a grid of calculated Debye specific-heat curves ( $C_v$ ) for Debye temperatures of 100–600 °K. Ignoring the peaks due to the antiferromagnetic-paramagnetic transition, a visual estimate gives Debye temperatures of 500, 400, and 300 °K for  $\text{FeF}_2$ ,  $\text{FeF}_3$ , and  $\text{FeCl}_2$ , respectively. One must remember that Mössbauer experiments measure the Debye (or Einstein) temperature for the dynamics of the  $\text{Fe}^{57}$  nucleus. However, in general one expects the higher-frequency lattice vibrations to be associated with the lighter anions ( $\text{F}^-$  or  $\text{Cl}^-$ ), with the result that the Debye temperature for  $\text{Fe}^{57}$  is expected to be lower than the Debye temperature for the lattice.<sup>27</sup> For example, the Mössbauer-measured  $\text{Fe}^{57}$  Debye temperature (1.29 times the Einstein temperature) for  $\text{FeF}_2$  of 450 °K is less than the estimated lattice Debye temperature of 500 °K, and similarly for  $\text{FeCl}_2$  the  $\text{Fe}^{57}$  Debye temperature of 180 °K is less than the lattice Debye temperature of 300 °K. Hence a Debye temperature for  $\text{Fe}^{57}$  of 615 °K in model (a) or 506 °K in model (b), which is larger than the lattice Debye temperature of 400 °K, is somewhat surprising. On the other hand, by assuming that the Debye temperature at  $\text{Fe}^{57}$  in  $\text{FeF}_3$  is less than the Debye temperature of  $\text{Fe}^{57}$  in  $\text{FeF}_2$ , we can explain our data with an  $\epsilon$  value for  $\text{FeF}_3$  greater than 4 mm/sec °K, compared with  $-1 \text{ mm/sec } ^\circ\text{K}$  for  $\text{FeF}_2$ . Hence the different behavior of  $\text{Fe}^{57}$  in  $\text{FeF}_3$  and  $\text{FeF}_2$  (or  $\text{FeCl}_2$ ) suggests that either the Debye temperature for  $\text{Fe}^{57}$  in  $\text{FeF}_3$  is larger than the lattice Debye temperature or  $\epsilon$  for  $\text{Fe}^{57}$  in  $\text{FeF}_3$  is greater than 4 mm/sec °K. This value for  $\epsilon$  is comparable with the calculated volume-expansion contribution to  $\epsilon$  for  $\text{FeF}_2$  of 5 mm/sec °K; however, a better estimate of the volume-expansion contribution to  $\epsilon$  for  $\text{FeF}_3$  may be 1.5 mm/sec °K<sup>8</sup> based on data for  $\text{K}_3\text{FeF}_6$ . In other words, assuming that the Debye temperature

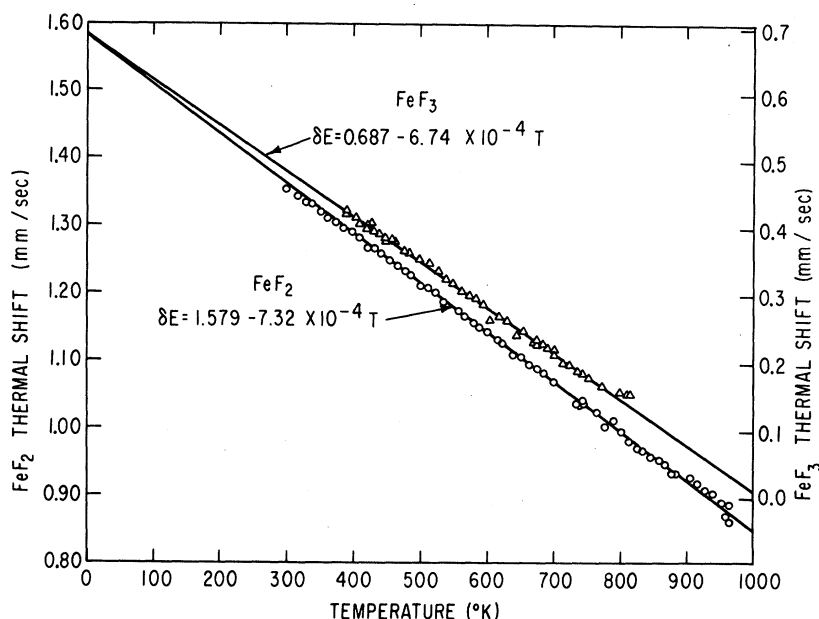


FIG. 10. Comparison of the Mössbauer resonance energy as a function of temperature for  $\text{FeF}_2$  and  $\text{FeF}_3$ . The experimental error increases from  $\pm 0.005$  mm/sec at 300 °K to  $\pm 0.010$  mm/sec at 960 °K.

for the  $\text{Fe}^{57}$  nucleus in  $\text{FeF}_3$  is not larger than the corresponding one in  $\text{FeF}_2$  (as indicated by the thermodynamic data), the difference between the two slopes in Fig. 10 indicates a significant thermal variation of  $\delta E_T$  in  $\text{FeF}_3$ .

#### V. DISCUSSION

Interpretation of our high-temperature Mössbauer quadrupole-splitting data leads us to estimate that the  $\text{FeF}_2$  axial contribution to the crystal field splitting decreases by one-fifth as the temperature increases from 300 to 960 °K. The magnitude of this decrease is consistent with the decrease in the axial distortion ( $d_4 - d_2$ ) calculated using the high-temperature x-ray data assuming constant  $u$ . The weak dependence of the quadrupole splitting on the smaller rhombic contribution to the crystal field furnishes no information on its temperature dependence; however, the x-ray data suggest that it also decreases at higher temperatures. The high-pressure quadrupole-splitting data of Champion *et al.* have been interpreted in this paper to indicate a higher-order phase transition around 65 kbar, based on the fact that the data can be fit by two straight lines differing in slope by a factor of 20. Since the unit-cell parameters ( $a, c$ ) vary smoothly with pressure, a plausible cause of this break is the failure of the assumption of constant  $u$ . We were successful in fitting the quadrupole splitting below 60 kbar by estimating the contribution due to radial expansion of the  $3d$  orbitals with increased pressure. This is in addition to the decrease in the splitting of the ferrous  $T_{2g}$  state with pressure previously considered by Christoe and Drickamer. Even though  $3d$  radial expansion has

been suggested to explain the increase in  $s$ -electron density at higher pressure (due to decreased shielding of the nucleus by the  $3d$  electrons)<sup>6</sup> no previous attempt has been made to estimate the effect. We have estimated this using the phenomenological relationship of Axtmann *et al.* for anhydrous ferrous halides. This enables us to use the pressure dependence of the isomer shift, which is assumed to depend on the change in  $\langle r^{-3} \rangle$  of the  $3d$  electron, to estimate the percentage decrease in  $\langle r^{-3} \rangle$ . In the case of  $\text{FeF}_2$ , the radial expansion accounts for 50% of the decrease in quadrupole splitting. Since all reported isomer shifts show a considerable decrease with increasing pressure, it is expected that changes in  $\langle r^{-3} \rangle$  contribute significantly to the pressure dependence of the quadrupole splitting in other  $\text{Fe}^{2+}$  compounds.

By subtracting the second-order Doppler shift from our thermal-shift data we show that the three  $\text{Fe}^{2+}$  compounds,  $\text{FeF}_2$ ,  $\text{KFeF}_3$ , and  $\text{FeCl}_2$  have essentially temperature-independent isomer shifts. This implies that the positive change in the isomer shift from increased volume (based on high-pressure data) is canceled by negative-explicit-temperature dependence of the isomer shift. For  $\text{FeF}_2$  sufficient data are available to calculate the expected linear coefficient due to volume expansion as  $5 \times 10^{-5}$  mm/sec °K and the resulting linear coefficient associated with the explicit  $-6 \times 10^{-5}$  mm/sec °K.

A comparison of the thermal shifts for  $\text{FeF}_3$  and  $\text{FeF}_2$  in the paramagnetic region ( $T > 370$  °K) shows for  $\text{FeF}_3$  a slope of  $-6.7 \times 10^{-4}$  mm/sec °K compared with the slope for  $\text{FeF}_2$  of  $-7.3 \times 10^{-4}$  mm/sec °K. In order to attribute this to a difference in the sec-

ond-order Doppler effect (instead of the temperature dependence of the isomer shift), the Debye temperature  $\Theta_D$  for  $\text{Fe}^{57}$  in  $\text{FeF}_3$  must be roughly twice the Debye temperature for  $\text{Fe}^{57}$  in  $\text{FeF}_2$  (approximately 600 and 300 °K, respectively). However, lattice-specific-heat data  $C_P$  for  $\text{FeF}_2$  and  $\text{FeF}_3$  indicate that the lattice Debye temperature for  $\text{FeF}_3$  is less than the lattice Debye temperature for  $\text{FeF}_2$  (approximately 400 and 500 °K, respectively). Since the Debye temperature for the  $\text{Fe}^{57}$  nucleus is expected to be less than the Debye temperature for the lattice, we do not expect a Debye temperature for  $\text{Fe}^{57}$  in  $\text{FeF}_3$  of 600 °K and, hence, cannot explain the thermal-shift slope without considering the temperature dependence of the isomer shift. Assuming that the Debye temperatures for  $\text{Fe}^{57}$  in  $\text{FeF}_2$  and  $\text{FeF}_3$  are equal, the difference in their thermal-shift slopes arises from a difference in the temperature dependence of their isomer shifts. (If the  $\text{Fe}^{57}$  Debye temperature were less in  $\text{FeF}_3$  than in  $\text{FeF}_2$ , this would increase the difference in the temperature dependence of their isomer shifts.)

The significant differences between the three ferrous compounds, which all have the  $\text{Fe}^{2+}$  ion octahedrally coordinated to the halide ions, are (a) the ferrous-chloride bond is more covalent than the ferrous-fluoride bond and (b) slight distortions from octahedral symmetry split the  $T_{2g}$  state in  $\text{FeF}_2$  and  $\text{FeCl}_2$  while it is unsplit in  $\text{KFeF}_3$ . Therefore, our experiments can measure no significant effect on the temperature dependence of the isomer shift that can be attributed to the thermal population of low-lying states or the difference in covalency in the ferrous-fluoride and ferrous-chloride bonds. Such a difference might be observable with a better estimate of the second-order Doppler contribution to the thermal shift. The  $\text{FeF}_3$  crystal structure<sup>28</sup> has the  $\text{Fe}^{3+}$  ion octahedrally surrounded by fluoride ions; however, the ferric-fluoride bonds are likely to have more 4s-electron involvement than the ferrous-fluoride bonds. The  $\text{Fe}^{3+}$  3d electron configuration is  $t_{2g}^3 e_g^2$ , while the  $\text{Fe}^{2+}$  3d-electron configuration is  $t_{2g}^4 e_g^2$ , i. e., a difference of one  $t_{2g}$  electron.

Now let us explore the consequences of a model which assumes (i) that the observed difference in the temperature dependence of the isomer shift for ferrous and ferric compounds results solely from the extra  $t_{2g}$  electron, and (ii) that the shielding of the nuclear charge by the 3d electrons is essentially the sum of the shielding produced by the  $t_{2g}$  electrons and the  $e_g$  electrons. Then the fact that  $(\partial\delta E_I/\partial T)_P$  for the  $t_{2g}^4 e_g^2$  configuration is essentially zero, while  $(\partial\delta E_I/\partial T)_P$  for the  $t_{2g}^3 e_g^2$  configuration is positive, implies an expansion of the  $t_{2g}$  radial wave function and a contraction of the  $e_g$  radial wave function with increasing temperature. These two effects cancel for the  $\text{Fe}^{2+}$  ion, while the ef-

fect of  $e_g$  radial contraction dominates for the  $\text{Fe}^{3+}$  ion. This model results in the opposite temperature dependence of the radial wave functions for the  $t_{2g}$  electrons and the  $e_g$  electrons.

Other models, which also have an expansion of the  $t_{2g}$  radial wave function and a contraction of the  $e_g$  radial function relative to the free ion (due to bonding), have recently been successful in explaining the neutron data for<sup>29</sup> CoO and the systematics of the Mössbauer data in high-spin ferrous compounds.<sup>30</sup> Similar behavior is found in metallic iron if one combines (a) the knowledge that the 3d radial wave functions associated with the top of its 3d band are contracted while those at the bottom of its 3d band are expanded<sup>31</sup> with (b) the fact, obtained from Fourier analysis of the magnetic-neutron-scattering data, that the magnetic electrons have predominantly  $e_g$  symmetry.<sup>32</sup> The symmetry of the unpaired spin-density distribution reflects the symmetry of the distribution of the unfilled portion at the top of the 3d band, which implies that the contracted 3d wave functions are predominantly of  $e_g$  character. This may imply a predominant  $t_{2g}$  symmetry for the expanded wave functions at the bottom of the 3d band.<sup>33</sup> Consequently, one should not be surprised if changes in bonding with temperature also affect the  $e_g$  and  $t_{2g}$  radial wave functions of the 3d electrons in opposite ways.

The pressure dependence of the Mössbauer isomer shift also shows a significant difference between the  $\text{Fe}^{2+}$  and  $\text{Fe}^{3+}$  compounds.<sup>6</sup> An analysis,

TABLE II.  $\text{FeCl}_2$  quadrupole-splitting data.

$T$ (°K)	$\Delta E_Q^a$ (mm/sec)	$T$ (°K)	$\Delta E_Q^a$ (mm/sec)	$T$ (°K)	$\Delta E_Q^a$ (mm/sec)
299	0.779	416	0.633	519	0.534
302	0.775	427	0.634	527	0.524
334	0.738	432	0.623	529	0.534
339	0.724	437	0.614	540	0.517
346	0.725	440	0.604	551	0.499
351	0.714	448	0.602	562	0.499
361	0.700	463	0.583	570	0.495
370	0.697	470	0.574	571	0.492
373	0.681	475	0.577	581	0.481
379	0.677	486	0.567	587	0.475
383	0.683	486	0.562	595	0.461
390	0.669	497	0.549	610	0.454
391	0.662	498	0.555	619	0.446
403	0.653	507	0.539	625	0.444
403	0.647	508	0.544	634	0.435
413	0.642	517	0.531	644	0.440

<sup>a</sup>The experimental error of  $\pm 0.007$  mm/sec arises from variation in the room-temperature quadrupole splitting with thermal history. A corresponding variation in the isomer shift was not observed. This variation in the quadrupole splitting could be associated with the formation of some metastable hexagonal close-packed phase, as discussed by MacLaren and Gregory (Ref. 34).

using assumptions similar to those used for the temperature dependence, implies that the radial wave function for the  $t_{2g}$  electron expands and the one for the  $e_g$  electron contracts with increasing pressure. The expansion of the  $t_{2g}$  radial wave function with both increased temperature (volume increase) and increased pressure (volume decrease) requires an explicit temperature dependence of the  $t_{2g}$  radial wave function. A similar argument holds for an explicit temperature dependence of the  $e_g$  radial wave function. The explicit temperature dependence of these radial wave functions, which results from the previously stated set of assumptions, supports the more general conclusion of this paper that the isomer shift has an explicit temperature dependence.

## ACKNOWLEDGMENTS

The authors wish to thank L. Crowder for experimental help, Dr. H. G. Guggenheim of Bell Telephone Laboratories for preparing the  $\text{FeF}_2$  sample, and Dr. Gerald Davidson of Bell Telephone Laboratories for sending us the  $\text{KFeF}_3$  sample. The authors acknowledge Professor R. C. Axtmann for useful discussions and suggestions throughout the course of this work. This work made use of the Princeton University Computer Center, supported in part by the National Science Foundation Grant Nos. NSF-GJ-34 and NSF-GU-3157.

## APPENDIX

The quadrupole-splitting data on  $\text{FeCl}_2$  are presented in Table II.

<sup>†</sup>Supported by the U. S. Atomic Energy Commission.

\*Sloan Postdoctoral Fellow.

<sup>‡</sup>Present address: Computer Center, Princeton University, Princeton, N. J. 08540.

<sup>1</sup>R. Ingalls, *Phys. Rev.* **133**, A787 (1964).

<sup>2</sup>U. Ganiel and S. Shtrikman, *Phys. Rev.* **177**, 503 (1969).

<sup>3</sup>D. P. Johnson and R. Ingalls, *Phys. Rev. B* **1**, 1013 (1970).

<sup>4</sup>C. W. Christoe and H. G. Drickamer, *Phys. Rev. B* **1**, 1813 (1970); C. W. Christoe, Ph. D. thesis (University of Illinois, 1969) (unpublished).

<sup>5</sup>Y. Hazony and H. K. Perkins, *J. Appl. Phys.* **41**, 5130 (1970).

<sup>6</sup>A. R. Champion, R. W. Vaughan, and H. G. Drickamer, *J. Chem. Phys.* **47**, 2583 (1967).

<sup>7</sup>R. C. Axtmann, Y. Hazony, and J. W. Hurley, Jr., *Chem. Phys. Letters* **2**, 673 (1968).

<sup>8</sup>G. K. Wertheim, D. N. E. Buchanan, and H. J. Guggenheim, *Phys. Rev. B* **2**, 1392 (1970).

<sup>9</sup>R. M. Housley and F. Hess, *Phys. Rev.* **146**, 517 (1966); **164**, 340 (1967).

<sup>10</sup>W. M. Walsh, Jr., Jean Jeener, and N. Bloembergen, *Phys. Rev.* **139**, A1338 (1965).

<sup>11</sup>K. N. Shrivastava, *Phys. Rev. B* **1**, 955 (1970).

<sup>12</sup>L. Neel, *Rev. Mod. Phys.* **25**, 58 (1953).

<sup>13</sup>J. W. Stout and S. A. Reed, *J. Am. Chem. Soc.* **76**, 5279 (1954); W. H. Baur, *Acta Cryst.* **11**, 488 (1958); J. W. Stout and R. G. Shulman, *Phys. Rev.* **118**, 1136 (1960).

<sup>14</sup>K. V. Krishna Rao, S. V. Nagender Naidu, and L. Lyengar, *Current Sci. (India)* **35**, 280 (1966).

<sup>15</sup>K. Siratori and S. Iida, *J. Phys. Soc. Japan* **17**, B1, 208 (1962). This paper reports that  $u$  changes with temperature in  $\text{CrO}_2$ , which also has a rutile crystal structure. Hence, this assumption of constant  $u$  is questionable.

<sup>16</sup>G. D. Jones, *Phys. Rev.* **155**, 259 (1967).

<sup>17</sup>G. K. Wertheim and D. N. E. Buchanan, *Phys. Rev.* **161**, 478 (1967); G. K. Wertheim, *ibid.* **121**, 63 (1961). (1961).

<sup>18</sup>A more generalized treatment would allow the Stern-

heimer factor to vary. In this case the isomer-shift change would be used to estimate the change in the product  $(1-R)\langle r^{-3} \rangle$ , and the numerical contribution from the variation in  $(1-R)\langle r^{-3} \rangle$  would be the same as calculated when all the variation was assumed to be due to  $\langle r^{-3} \rangle$ .

<sup>19</sup>A. F. Wells, *Structural Inorganic Chemistry* (Oxford U. P., Oxford, 1962); K. Knox, *Acta Cryst.* **14**, 583 (1961).

<sup>20</sup>A. Okazaki and Y. Suemune, *J. Phys. Soc. Japan* **16**, 671 (1961).

<sup>21</sup>Y. Hazony, R. C. Axtmann, and J. W. Hurley, Jr., *Bull. Am. Phys. Soc.* **15**, 106 (1970).

<sup>22</sup>D. P. Johnson and J. G. Dash, *Phys. Rev.* **172**, 983 (1968).

<sup>23</sup>K. K. Kelley and G. E. Moore, *J. Am. Chem. Soc.* **65**, 1264 (1943).

<sup>24</sup>K. Ono, A. Ito, and T. Fujita, *J. Phys. Soc. Japan* **19**, 2119 (1964).

<sup>25</sup>H. Bizette, R. Mainard, and J. Picard, *Compt. Rend.* **260**, 5508 (1965).

<sup>26</sup>E. Catalano and J. W. Stout, *J. Chem. Phys.* **23**, 1803 (1955).

<sup>27</sup>Ya. A. Iosilevskii, *Zh. Eksperim. i Teor. Fiz.* **54**, 927 (1968) [*Sov. Phys. JETP* **27**, 495 (1968)].

<sup>28</sup>M. A. Hepworth, K. H. Jack, R. D. Peacock, and G. J. Westland, *Acta Cryst.* **10**, 63 (1957).

<sup>29</sup>D. C. Khan and R. A. Erickson, *Phys. Rev. B* **1**, 2243 (1970).

<sup>30</sup>Y. Hazony, *Phys. Rev. B* **3**, 711 (1971); Y. Hazony, in *Advances in Mössbauer Effect Methodology*, edited by I. Gruverman (Plenum, New York, to be published), Vol. 7.

<sup>31</sup>R. Nathans, S. J. Pickart, and H. A. Alperin, *J. Phys. Soc. Japan Suppl.* **17**, 7 (1962).

<sup>32</sup>C. G. Shull and Y. Yamada, *J. Phys. Soc. Japan Suppl.* **17**, 1 (1962).

<sup>33</sup>This possible similarity between the situation in metallic iron and high-spin ferrous compounds was suggested by R. Ingalls (private communication).

<sup>34</sup>R. O. MacLaren and N. W. Gregory, *J. Am. Chem. Soc.* **76**, 5874 (1954).